



Characterizing spectral–temporal patterns of defoliator and bark beetle disturbances using Landsat time series



Cornelius Senf^{a,*}, Dirk Pflugmacher^a, Michael A. Wulder^b, Patrick Hostert^{a,c}

^a Geography Department, Humboldt-Universität zu Berlin, Unter den Linden 6, 10099 Berlin, Germany

^b Canadian Forest Service (Pacific Forestry Centre), Natural Resources Canada, 506 West Burnside Road, Victoria, BC V8Z 1M5, Canada

^c Integrative Research Institute on Transformations of Human-Environment Systems (IRI THESys), Humboldt-Universität zu Berlin, Unter den Linden 6, 10099 Berlin, Germany

ARTICLE INFO

Article history:

Received 12 March 2015

Received in revised form 11 September 2015

Accepted 23 September 2015

Available online xxxx

Keywords:

Landsat

Time series

Insect disturbances

Defoliation

Western spruce budworm (*Choristoneura freemani* Razowski)

Bark beetles

Mountain pine beetle (*Dendroctonus ponderosae* (Hopkins))

LandTrendr

British Columbia

ABSTRACT

Defoliators and bark beetles are natural disturbance agents in many forest ecosystems around the world. Mapping the spatial and temporal patterns of insect disturbance dynamics can help in understanding their impacts on forest ecosystem resilience and functioning, and in developing adaptive management strategies. In recent years, much progress has been made in landscape-level analyses of insect-induced disturbances using remotely sensed data. However, many studies have focused on single insect agents or aggregated different insect agents into a single group. In this study, we characterized the temporal-spectral patterns associated with bark beetle and defoliator disturbances using Landsat time series between 1990 and 2013, with the objective to test if the two insect disturbances can be separated with Landsat data. We analyzed a recent outbreak of mountain pine beetle (*Dendroctonus ponderosae* Hopkins) and western spruce budworm (*Choristoneura freemani* Razowski) in British Columbia, Canada. To characterize the disturbance and recovery trends associated with insect disturbances we used the LandTrendr segmentation algorithm. We fitted LandTrendr spectral trajectories to annual normalized burn ratio (NBR) and Tasseled Cap (TC) time series, from which we then extracted a set of disturbance metrics. With these disturbance metrics, two random forest models were trained to a) distinguish insect disturbances from harvest and fire disturbances; and to b) attribute the insect disturbances to the most likely agent, i.e. mountain pine beetle or western spruce budworm. Insect disturbances were successfully mapped with an overall accuracy of 76.8%, and agents were successfully attributed with overall accuracies ranging from 75.3% to 88.0%, depending on whether only pure host-stands or mixed stands with both insect hosts were considered. In the case of mixed host stands, nearly 45% of the western spruce budworm disturbances were falsely attributed to mountain pine beetle. Spectral metrics describing disturbance magnitude were more important for distinguishing the two insect agents than the disturbance duration. Spectral changes associated with western spruce budworm disturbances had generally lower magnitudes than mountain pine beetle disturbances. Moreover, disturbances by western spruce budworm were more strongly associated with changes in TC greenness, whereas disturbances by mountain pine beetle were more strongly associated with changes in TC brightness and wetness. The results reflect the ephemeral nature of defoliators versus the tree mortality impacts of bark beetles in our study area. This study demonstrates the potential of Landsat time series for mapping bark beetle and defoliator disturbances at the agent level and highlights the need for distinguishing between the two insect agents to adequately capture their impacts on ecosystem processes.

© 2015 Elsevier Inc. All rights reserved.

1. Introduction

Insect disturbances play an important role in forest ecosystem dynamics by renewing old and susceptible forests, recycling nutrients, and providing food for wildlife (Parker, Clancy, & Mathiasen, 2006). There is increasing evidence that human actions through management and climate change have altered the interactions between insects and forests, resulting in more widespread insect outbreaks (Raffa et al., 2008; Schoennagel, Veblen, & Romme, 2004; Swetnam & Lynch, 1993).

Using climate change projections, current research indicates that outbreaks will become more frequent in the future (Logan, Régnière, & Powell, 2003; Volney & Fleming, 2000; Woods, Heppner, Kope, Burleigh, & Maclauchlan, 2010), which will have significant consequences for the future carbon balance of forests (Hicke et al., 2012; Kurz et al., 2008a; Kurz, Stinson, Rampley, Dymond, & Neilson, 2008b).

Monitoring insect outbreaks with remote sensing data systematically over space and time can help with understanding landscape-scale causes and consequences of insect disturbances. Two of the most prevalent insect agents causing widespread tree damage and mortality are bark beetles and defoliators. Since impacts of defoliators and bark beetles on ecosystem function and structure are different (Hicke et al., 2012),

* Corresponding author.

E-mail address: cornelius.senf@geo.hu-berlin.de (C. Senf).

distinguishing between insect agents is important to adapt forest management strategies and to improve ecosystem process models. However, studies mapping insect disturbances over large areas usually group defoliators and bark beetles into a single disturbance category (Huang et al., 2010; Kennedy et al., 2012; Masek et al., 2013).

In coniferous forests of North America, the most important bark beetle is the mountain pine beetle (*Dendroctonus ponderosae* Hopkins). Mountain pine beetles reproduce in the phloem below the bark and introduce a fungus, which clogs the phloem and limits the translocation of water and nutrients through the tree. By using pheromones, the beetles usually follow a cooperative behavior strategy (mass attack) to help overcome the defensive system of trees. Attacks by mountain pine beetle are not noticeable in the first year of infestation (green-attack stage) but typically lead to complete discoloration (red-attack stage) in the second year and complete defoliation (gray-attack stage) in the third year (Wulder, Dymond, White, Leckie, & Carroll, 2006a). However, the progression of infestation by mountain pine beetle can vary by region, site, and species (Wulder et al., 2006a).

In comparison to bark beetles, defoliating insects cause mild to moderate disturbances (Cooke, Nealis, & Regniere, 2007). The most prominent defoliators in coniferous forests of North America are in the genus *Choristoneura* (spruce budworm), including the eastern spruce budworm (*Choristoneura fumiferana* Clemens), the jack pine budworm (*Choristoneura pinus pinus* Freeman), the western spruce budworm (*Choristoneura freemani* Razowski), the 2-year-cycle spruce budworm (*Choristoneura biennis* Free.), and the coastal spruce budworm (*Choristoneura orae* Free.) (Nealis, 2008). From those, the western spruce budworm is most important for western North America (Hicke et al., 2012). Western spruce budworm larvae feed primarily on current-year foliage, which can lead to chlorosis, crown dieback, and tree death; particularly when insect populations are high over several years and in cases of secondary infestation by bark beetles (Alfaro, Thomson, & Van Sickle, 1984; Alfaro, Van Sickle, Thomson, & Wegwitz, 1982; Shepherd, 1994). Nonetheless, if defoliation rates are low, most trees typically will experience little damage and recover within several years (Campbell, Smith, & Arsenault, 2006; Shepherd, 1994). Western spruce budworm outbreaks return every 30 years on average, though the intensity of outbreaks can vary significantly (Alfaro, Berg, & Axelsson, 2014; Axelsson, Smith, Daniels, & Alfaro, 2015).

Previous studies have shown that Landsat's spectral bands can be used to discriminate healthy forests from insect disturbed forests. Also, with a 30 m spatial resolution, Landsat operates at a scale that is informative for ecological research and management decisions (Cohen & Goward, 2004; Wulder et al., 2008). Early studies utilizing Landsat for insect disturbance mapping in coniferous forests typically used spectral information from one or two images, including the Tasseled Cap components (Franklin, Waring, McCreight, Cohen, & Fiorella, 1995; Skakun, Wulder, & Franklin, 2003), spectral bands (Franklin, Wulder, Skakun, & Carroll, 2003), spectral mixture analysis (Radeloff, Mladenoff, & Boyce, 1999), and vegetation indices based on near-infrared and shortwave-infrared reflectance (Franklin, Fan, & Guo, 2008). However, approaches based on single years and binary maps are somewhat restricted in characterizing the complex ecological dynamics of insect outbreaks. Thus, a more comprehensive mapping approach is needed, utilizing as many points in time as possible and characterizing the disturbance magnitude and duration (Gillanders, Coops, Wulder, Gergel, & Nelson, 2008; Kennedy et al., 2014).

Following the opening of the United States Geological Survey (USGS) Landsat archive and the related increase in capacity to produce time series (Wulder, Masek, Cohen, Loveland, & Woodcock, 2012), annual Landsat time series were successfully used in a number of studies to capture insect-infestation. While implemented just prior to the opening of the USGS archive, Goodwin et al. (2008) used annual Landsat time series to capture infestation by mountain pine beetle in British Columbia. In this study, spectral trajectories displayed little to no change in the first year of infestation, but a decreasing trend in subsequent years.

Similar spectral and temporal trends were found for mountain pine beetle in Montana (Assal, Sibold, & Reich, 2014), in Colorado (Meddens & Hicke, 2014), and in Oregon (Meigs, Kennedy, & Cohen, 2011). The changes in Landsat spectral trajectories were linked to tree mortality (Meigs et al., 2011; Pflugmacher, Cohen, & Kennedy, 2012), which enabled a landscape-scale assessment of mountain pine beetle impacts (Bright, Hudak, Kennedy, & Meddens, 2014; Meigs, Kennedy, Gray, & Gregory, 2015). Defoliator disturbances were also associated with gradual changes in the spectral signal (Meigs et al., 2011; Vogelmann, Tolk, & Zhu, 2009; Vogelmann, Xian, Homer, & Tolk, 2012), but spectral trajectories were highly variable. Changes during defoliation were explained by decreasing vigor, top-kill, and increasing mortality resulting from consecutive defoliation events, though many trajectories also showed quick spectral recovery after disturbance. Thus, recent studies suggest that Landsat time series can be utilized to characterize the complex spatial and temporal dynamics of insect outbreaks, but spectral trajectories vary considerable among insect agents, regions, and outbreak intensities. To better understand the ecological dynamics of insect disturbances, a better understanding of the spectral-temporal trajectories of individual insect agents is needed, enabling a more detailed mapping of insect disturbances – i.e. by distinguishing between bark beetle and defoliator disturbances.

Here, our goal was to determine the capacity of spectral-temporal trajectories from annual Landsat time series to map defoliator and bark beetle disturbance dynamics in southern-interior British Columbia, Canada. Our specific objectives were to:

1. Test how well bark beetle and defoliator disturbances can be distinguished with Landsat time series.
2. Characterize the spectral-temporal trajectories of bark beetle and defoliator disturbances with respect to severity, duration, and spectral recovery.
3. Map the spatial and temporal pattern of mountain pine beetle and western spruce budworm disturbances.

2. Study site

Our study site is located in the interior of British Columbia, Canada, occupying an area of approximately 149,700 km². The outer extent of the study site (hereafter referred to as *Interior*) is delineated by eight Landsat footprints (WRS-2 path/row: 45/25, 45/26, 46/24, 46/25, 46/26, 47/24, 47/25, 48/24; Fig. 1). In British Columbia, a province-wide biogeoclimatic classification system has been established that describes the natural ecozones based on climatic and vegetation characteristics (Pojar, Klinck, & Meidinger, 1987). The Interior is dominated by the Interior Douglas-fir Forest zone (Hope et al., 1991). The Interior Douglas-fir Forest zone is characterized by mature Douglas-fir (*Pseudotsuga menziesii* (Mirb.) Franco) stands at mid-elevations (900–1200 m), mixed stands of Douglas-fir and ponderosa pine (*Pinus ponderosa* Douglas ex C. Lawson) at lower elevations (600–900 m), and mixed stands of Douglas-fir and lodgepole pine (*Pinus contorta* Douglas) at higher elevations (1200–1450). The Interior Douglas-fir Forest borders the Montane Spruce zone at higher elevations, which is actually a transition zone to the Engelmann Spruce and Subalpine Fir zone. In the Interior, the Montane Spruce zone is characterized by extensive seral stands of lodgepole pine. At lower elevations, the Interior Douglas-fir Forest borders the Ponderosa Pine zone, which is dominated by open stands of ponderosa pine. In the northern part of the study site, the Interior Douglas-fir Forest borders the Sub-Boreal Pine and Spruce zone. The Sub-Boreal Pine and Spruce zone is dominated by lodgepole pine. The very low elevation areas are part of the largely non-treed bunchgrass zone.

The Interior and in particular the Interior Douglas-fir Forest have experienced a complex history of fire and insect disturbances (Campbell et al., 2006; MacLachlan, Brooks, & Hodge, 2006). There are records of western spruce budworm outbreaks over the past 400 years,

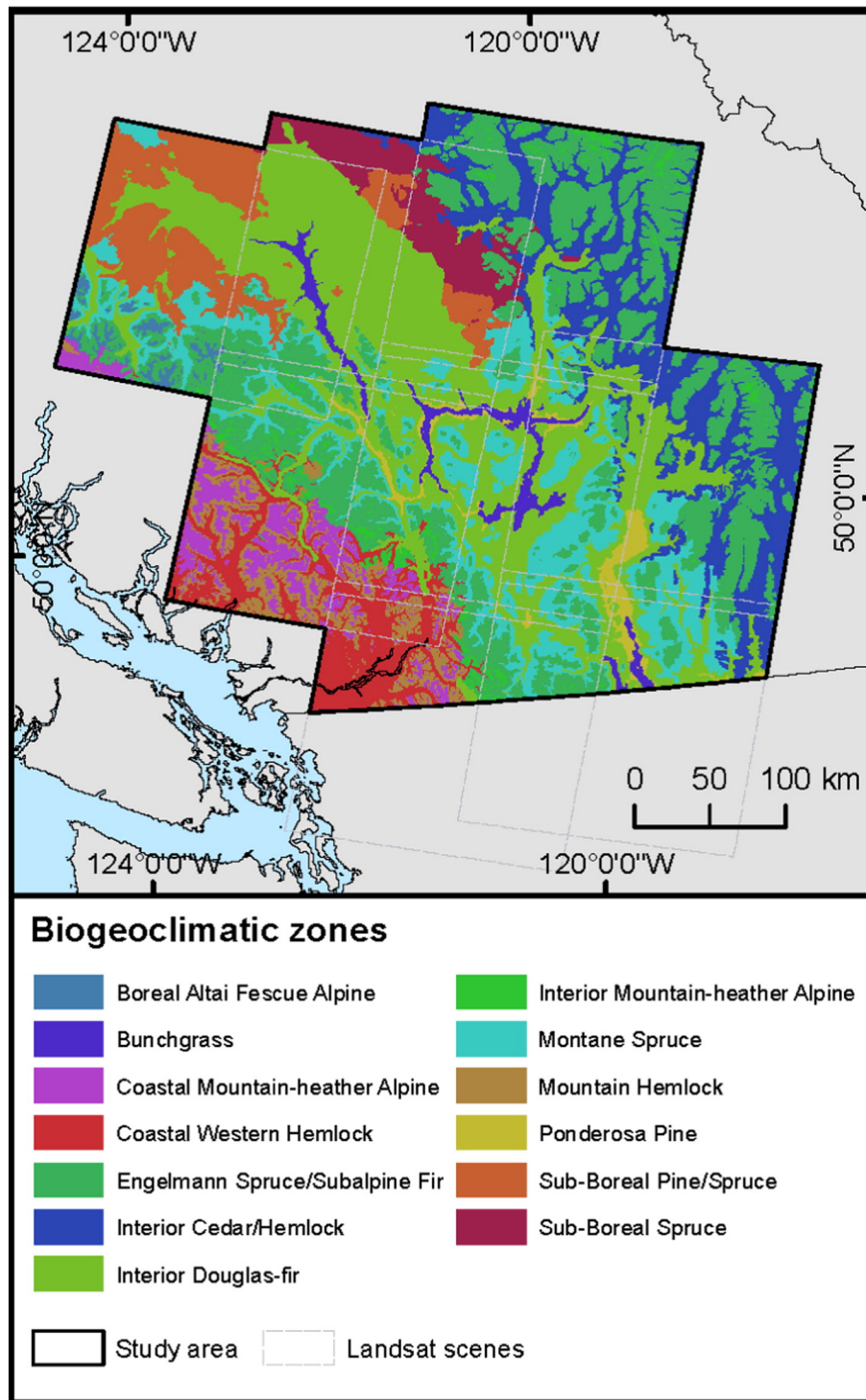


Fig. 1. Study area in British Columbia. The main map shows the major biogeoclimatic zones (BEC zones) in the study area.

although outbreak frequency has increased markedly during the past century (Campbell et al., 2006). The most recent outbreak from 1999 to 2012 affected the whole IDF and peaked in 2007 at approximately one million hectares of defoliated trees. It was the largest outbreak in recorded history (Westfall & Ebata, 2012). In British Columbia, western spruce budworm mainly feeds on Douglas-fir and true fir, though other species such as hemlock, Engelmann spruce, larch, and pine might occasionally be attacked if growing on site (Maclauchlan et al., 2006).

Mountain pine beetle is also active in the Interior. The most recent outbreak occurred between 2002 and 2012 and led to high mortality rates in ponderosa and lodgepole pine stands (Westfall & Ebata, 2012).

Even though mountain pine beetle can feed on any pine species, lodgepole-pine is considered its primary host in British Columbia (Wulder et al., 2006a).

3. Data and methods

3.1. Landsat data and LandTrendr disturbance mapping

We used the LandTrendr segmentation approach (Kennedy, Yang, & Cohen, 2010) to map and characterize disturbances between 1990 and 2013. To achieve this, we followed three main steps: 1) create annual

time series of cloud-free, anniversary-date observations; 2) fit time series trajectories for each pixel; and 3) derive a set of metrics from each trajectory to describe the disturbance and recovery characteristics of each pixel. We processed all Landsat footprints individually in their original UTM projection (WGS84) and then mosaicked the final disturbance metrics for the whole study site in the BC Albers Equal Area (NAD83) projection. For mosaicking, we used Voronoi polygons as edge lines between neighboring scenes (Kennedy et al., 2012). Areas that were non-forest in 1990 were masked out using a binary forest cover map created from supervised classification.

To minimize the effect of phenology and data gaps caused by atmospheric interference, LandTrendr builds annual anniversary-date, best observation composites using all cloud-free observations from each scene and overlapping scenes within a pre-defined seasonal window (Kennedy et al., 2010). We downloaded all available Landsat Thematic Mapper (TM) and Enhanced Thematic Mapper Plus (ETM+) scenes from the US Geological Survey (USGS) archive and used the LEDAPS algorithm (Masek et al., 2006) to produce surface reflectance images for the 23-year time period. For building the best observation composites, we defined the seasonal window as ± 30 days around July 15th. Clouds, cloud shadows, and snow were detected and masked out using the Fmask algorithm (Zhu & Woodcock, 2012).

Once a consistent annual time series is created, the LandTrendr algorithm fits spectral trajectories to the time series by dividing it into a series of connected linear segments following two main steps: First, the start and end of each segment is determined by estimating the years of change using a spectral index of choice (segmentation process). Second, the spectral index values at vertices are estimated (fitting process), yielding a trajectory of interconnected segments that characterize the disturbance history for each pixel (Fig. 2). The segment breakpoints are called vertices. In this study, we used the Normalized Burn Ratio (NBR) (Key & Benson, 2006) to derive the segmentation and then applied the fitting to NBR and the first three Tasseled Cap (TC) components (Crist, 1985). NBR has previously been demonstrated to be sensitive to insect disturbances in North America (e.g. De Beurs & Townsend, 2008; Meigs et al., 2011; Townsend et al., 2012) and has been used with LandTrendr in other studies (Kennedy et al., 2010; Kennedy et al., 2012; Meigs et al., 2011). However, NBR is only a single spectral index based on two bands, whereas the TC components are multi-dimensional indices derived from the multispectral data space. The TC components are sensitive to green vegetation abundance and vigor (greenness), canopy structure and moisture (wetness), and background soil signal (brightness) (Cohen & Goward, 2004) and have been used in many studies mapping insect infestation (e.g., Coops, Wulder, & White, 2006b; Skakun et al., 2003; Wulder, White, Bentz, Alvarez, & Coops, 2006b).

Finally, we derived a set of metrics describing the spectral-temporal characteristics of the trajectory fitted to NBR and TC trajectories, closely following Meigs et al. (2011) and Pflugmacher, Cohen, Kennedy, and Yang (2014). For each pixel's trajectory, we first identified the greatest disturbance segment, defined as the segment

with the greatest negative change in NBR. From the greatest disturbance segment, we calculated the change magnitude (GDMAG; Fig. 2), segment duration (GDDUR; Fig. 2), and recorded the onset of disturbance, defined as the first year of the greatest disturbance segment. Similarly, we calculated recovery magnitude (RCMAG; Fig. 2) and duration (RCDUR; Fig. 2) from the spectral recovery segment following the greatest disturbance segment. To facilitate interpretation, the NBR change magnitudes of disturbance and recovery were converted to percent change relative to the spectral value of the pre-disturbance condition (start vertex of each segment).

3.2. Mapping approach

We followed a two-phase classification approach to map spatial and temporal patterns of mountain pine beetle and western spruce budworm disturbances (Goodwin et al., 2008; Meigs et al., 2015): First, we classified the LandTrendr disturbance and recovery metrics into harvest and fire disturbances, insect disturbances, and undisturbed areas. We refer to this classification phase as *disturbance classification*. Second, we assigned all pixels identified as insect disturbances in the first classification phase a likelihood of being disturbed by either mountain pine beetle or western spruce budworm (in the following referred to as *insect agent attribution*).

3.2.1. Phase one: disturbance classification

In the first classification phase, we used the LandTrendr disturbance metrics to classify forest changes into 1) insect disturbances, 2) harvest and fire disturbances, and 3) undisturbed forest. Clear-cut harvest and fires behave differently in spectral and temporal space than insect disturbances, which makes them distinguishable with Landsat time series (Goodwin et al., 2008; Kennedy et al., 2012; Meigs et al., 2015). While insect disturbance can lead to complete stand mortality, spectral change magnitudes associated with harvest and fire disturbances are usually significantly higher (Goodwin et al., 2008; Hais, Jonášová, Langhammer, & Kučera, 2009), and of shorter duration (Meigs et al., 2015). As reference data, we randomly selected and labeled 800 pixels closely following the approach by Cohen, Yang, and Kennedy (2010); Kennedy et al. (2012); Pflugmacher et al. (2012) and Meigs et al. (2015).

For identifying and labeling disturbances in the reference pixels, we used Landsat image chips, Landsat spectral trajectory plots, high-resolution imagery, the provincial aerial overview survey (AOS) database (Wulder et al., 2009), the provincial Vegetation Resource Inventory (VRI) database (Leckie & Gillis, 1995), and the Canadian National Fire Database. The AOS collects polygon-level data on insect agent and disturbance severity during aerial overflights. The AOS (Fig. 7) is currently the most comprehensive database on insect disturbances at the landscape level (Meddens, Hicke, & Ferguson, 2012), but it is not a precise spatial product as it has several positional and attribution limitations, and it is subject to a certain observer bias, such as off-nadir viewing, variations in lighting conditions, and interpreter experience and fatigue, among others (Wulder et al., 2006a). To reduce uncertainties in the AOS data, we omitted polygons with the severity class 'trace', indicating only single infested trees within a stand (Wulder et al., 2009). Moreover, we only included insect disturbed pixels within mountain pine beetle and western spruce budworm host-tree stands according to the VRI. Stands in the VRI are delineated using very-high-resolution imagery, and species composition is assigned using photo interpretation (Leckie & Gillis, 1995). Species composition information includes the six leading species including their relative abundance. In total, 358 pixels were undisturbed, 145 were disturbed by harvest or fire, and 267 pixels were disturbed by insects (either mountain pine beetle or western spruce budworm). A small proportion (30 pixels) could not clearly be assigned to one of the three categories, and those were excluded from further analyses. In Fig. 3 we present examples of all three disturbances classes.

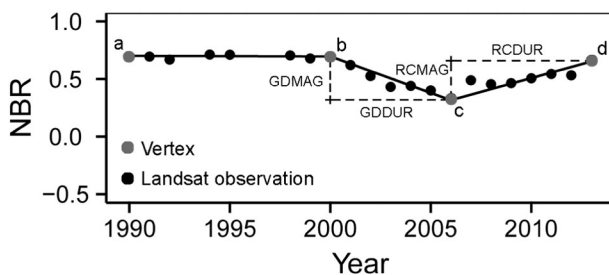


Fig. 2. Exemplified LandTrendr segmentation and spectral trajectory fitted to an NBR time series. Gray dots (a–d) indicate vertices. Disturbance and recovery metrics derived from the trajectory are shown.

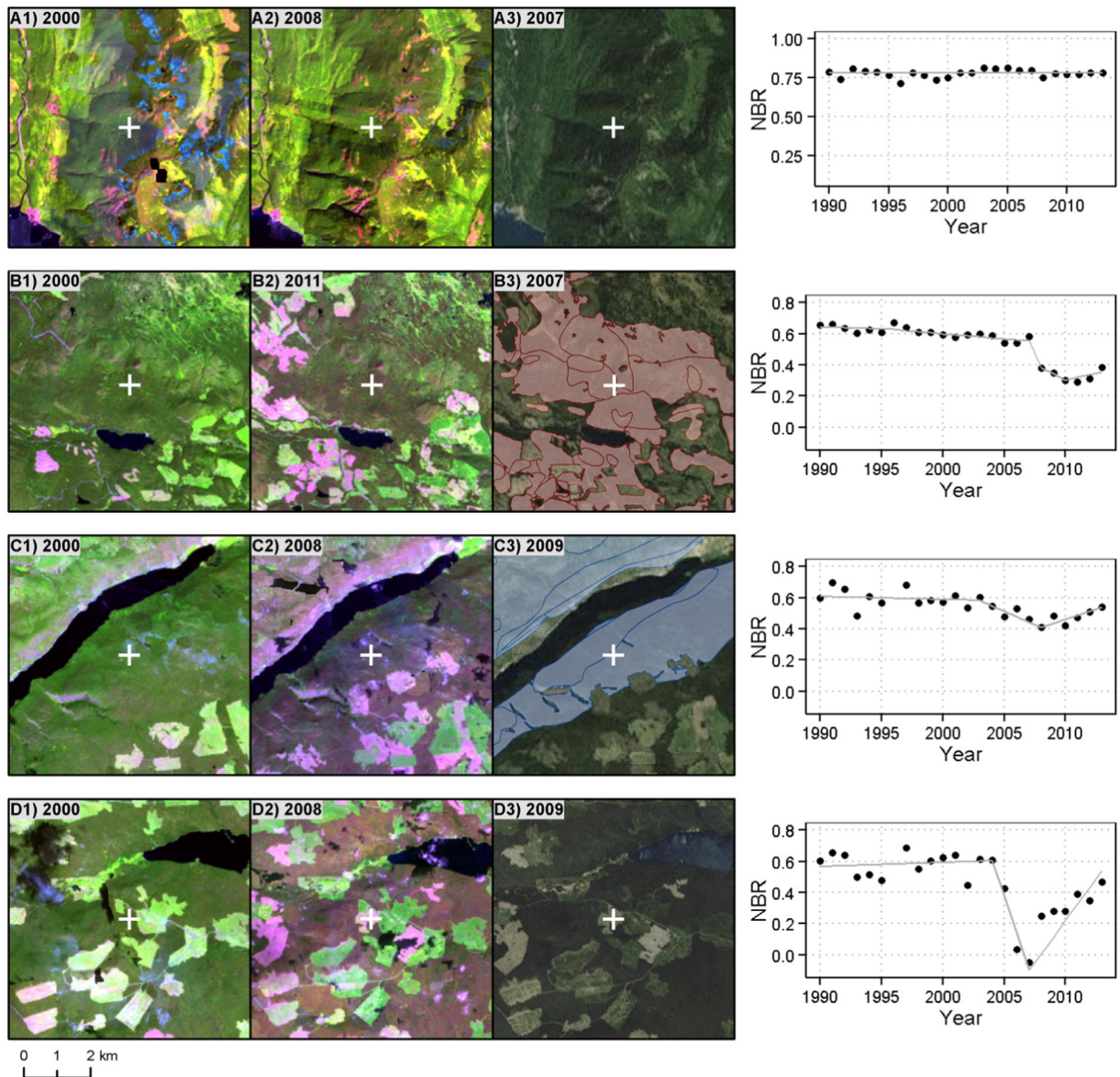


Fig. 3. Four examples of Landsat spectral trajectories (black dots) and LandTrendr fitted trajectories (gray lines) with corresponding Landsat image chips (columns one and two; R/G/B = Landsat band 4/5/3) and very high-resolution imagery (column three). For mountain pine beetle and western spruce budworm disturbances (rows B and C) the AOS polygons also are shown.

Using the reference pixels, we trained a random forest classification model (Breiman, 2001) provided in the *randomForest* package (Liaw & Wiener, 2002) of the statistical software R (R Core Team, 2014). The random forest model was validated using the out-of-bag confusion matrix (Breiman, 2001), from which we estimated overall, user's, and producer's accuracies, as well as errors of omission and commission.

3.2.2. Phase two: insect agent attribution

Following the disturbance mapping in phase one (Section 3.2.1), we estimated for each insect-disturbed pixel the probability of being disturbed by mountain pine beetle or western spruce budworm, respectively. Continuous probabilities of class presence offer greater flexibility in interpreting map predictions than discrete classes, i.e., by choosing more conservative or relaxed estimates of the total area disturbed (Wulder et al., 2006b). For this purpose, we calibrated a second random forest model with a second reference dataset based on the AOS and the VRI database. We selected all insect disturbance pixels covered by either a mountain pine beetle or a western spruce budworm AOS polygon, again omitting the 'trace' class. Some areas (16% of all pixels) were

covered by mountain pine beetle and western spruce budworm polygons, and we omitted those pixels from the reference set to avoid confusion between both insects. For model training, we further narrowed down the selection to those pixels identified as pure mountain pine beetle or western spruce budworm host-stands in the VRI (i.e. 100% Douglas-fir or 100% lodgepole pine), reducing unrelated spectral variability in the reference data (Franklin et al., 2003). From this selection, we randomly drew 10,000 pixels for training of a random forests model as described in Section 3.2.1; and sampled 10,000 pixels for validating the model in pure stands. Moreover, we sampled a second reference set of 10,000 pixels, covering pure and mixed stands. Using two reference sets – i.e. one sampled in pure host stands and one sampled independently of host-configuration – allowed us to assess the effects of mixed stands on attribution accuracy.

Using the trained random forest model, we predicted the probability of mountain pine beetle and western spruce budworm disturbances for all insect disturbance pixels. In random forest, the probability of class membership is estimated from the proportion of tree votes obtained by a class.

4. Results

4.1. Classification of disturbances and insect agents

The disturbance classification yielded an overall accuracy of 76.8% (Table 1), with the highest user's and producer's accuracies in the harvest/fire disturbance class (80.9% and 84.8%, respectively), slightly lower user's and producer's accuracies for the undisturbed class (78.8% and 83.2%, respectively), and moderate accuracies for the insect disturbance class (70.8% and 63.7%, respectively). Class confusion was highest between insect disturbances and undisturbed areas. In total, $34 \pm 9\%$ of the forested area was disturbed by insects and $20 \pm 9\%$ were disturbed by harvest or fire. Most of the forested area in the study area ($46 \pm 6\%$) was stable over the study period. The classification map (Fig. 4) was used to mask out undisturbed areas and harvest/fire disturbances in the following results.

The binary classification of mountain pine beetle and western spruce budworm disturbances (using a probability threshold of $p = 0.5$) achieved an overall accuracy of 88.0% in pure host-stands (Table 2), indicating that the two insects can be reliably distinguished using disturbance and recovery metrics derived from Landsat time series. Nonetheless, the overall accuracy dropped to 75.3% when mixed stands were considered (Table 3), suggesting that the attribution of insect agents is more difficult in stands composed of different host tree species. For pure stands (Table 2), the producer's and user's accuracies were well balanced between both insects, whereas the user's accuracy for mountain pine beetle disturbances was substantially lower (55.9%) for the mixed stands, which means that mountain pine beetle infected areas were overestimated in those stands.

4.2. Spectral–temporal characteristics of mountain pine beetle and western spruce budworm disturbances

Some differences between mountain pine beetle and western spruce budworm disturbances were apparent when comparing the disturbance and recovery metrics (Fig. 5). Disturbance magnitudes in NBR for mountain pine beetle were on average 20% higher than for western spruce budworm. For mountain pine beetle 50% of the disturbances had a disturbance magnitude higher than 40%, whereas for western spruce budworm this was only the case for 30% of the disturbances. The TC components showed more distinct differences between mountain pine beetle and western spruce budworm disturbances magnitudes (Fig. 6). Western spruce budworm disturbances showed a 30% higher decline in greenness than mountain pine beetle disturbances; whereas mountain pine beetle disturbances showed a three times higher decline in brightness than western spruce budworm. Moreover, mountain pine beetle disturbances showed a slightly higher increase in wetness during disturbance than western spruce budworm. This finding suggests that the TC components are of particular importance for separating between defoliator and bark beetle disturbances.

Differences in disturbance duration were not as distinct, though some general patterns could be observed (Fig. 5): For mountain pine beetle, 50% of the disturbances were very short (two years or less), 20% of the disturbances were between three and five years in duration,

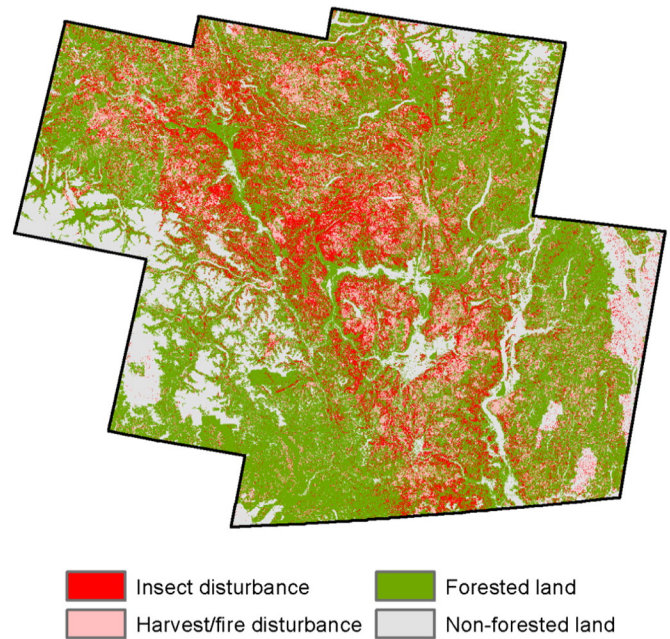


Fig. 4. Map derived in the disturbance classification phase showing undisturbed areas, harvest/fire disturbances, and insect disturbances. A binary map of the insect disturbances is later used to mask out undisturbed areas and areas disturbed by harvest/fire (Fig. 7).

and 30% of the disturbances persisted longer than 5 years. In comparison, western spruce budworm disturbances were only slightly longer on average (five years compared to four years for mountain pine beetle), though the proportion of long-duration (>5 years) disturbances was higher (40%). Only 20% of the western spruce budworm disturbances were between three and five years, and the remaining 40% were two years or shorter.

Differences in NBR recovery magnitude (Fig. 5) were not as distinct as differences for disturbances, with mountain pine beetle experiencing a slightly higher variation in recovery magnitude. For recovery duration, however, western spruce budworm disturbances resulted in longer recovery durations compared to those following mountain pine beetle disturbances. For the TC recovery magnitudes (Fig. 6), western spruce budworm and mountain pine beetle disturbed stands tended to completely recover in TC greenness. For spectral recovery in wetness, both insects had lower spectral recovery values than the changes in wetness during disturbance. Recovery in brightness was close to the changes during disturbance for mountain pine beetle and close to zero for western spruce budworm.

4.3. Spatial and temporal pattern of mountain pine beetle and western spruce budworm disturbances

The maps of mountain pine beetle and western spruce budworm disturbance probability (Fig. 7) resembled the disturbance patterns of the aerial overview survey quite well, although the spatial detail is

Table 1

Validation of the first classification phase (disturbance classification), which distinguishes undisturbed areas, insect disturbances, and clear-cut harvest and fire disturbances. The confusion matrix is derived from the out-of-bag sample of the random forest model.

		Reference					
Map	Class	Undisturbed	Insect	Harvest/fire	Total	User's accuracy [%]	Error of commission [%]
	Undisturbed	298	74	6	378	78.8	21.2
	Insect	54	170	16	240	70.8	29.2
	Harvest/fire	6	23	123	152	80.9	19.1
	Total	358	267	145			
	Producer's accuracy [%]	83.2	63.7	84.8		Overall accuracy [%]	
	Error of omission [%]	16.8	36.3	15.2		76.8	

Table 2
Confusion matrix for predicting mountain pine beetle (MPB) and western spruce budworm (WSBW) disturbances in pure host-stands.

		Reference				
Map	Agent	WSBW	MPB	Total	User's accuracy [%]	Error of commission [%]
	WSBW	4996	563	5559	89.9	10.1
	MPB	636	3805	4441	85.7	14.3
	Total	5632	4368			
	Producer's accuracy [%]	88.7	87.1		Overall accuracy [%]	
	Error of omission [%]	11.3	12.9		88.0	

much higher. Some differences can be found for mountain pine beetle in the northwestern part of the study area, though this area has also been subject to intensive salvage logging and fire (Fig. 4). High probabilities of mountain pine beetle disturbances are concentrated in the lodgepole pine dominated area in the northeastern part of the study site (Sub-boreal Pine and Spruce zone and Sub-boreal Spruce zone), and in the higher elevation regions of the Montane Spruce zone. High probabilities of western spruce budworm disturbances are concentrated in lower-elevation parts of the Douglas-fir dominated areas (Interior Douglas-fir zone) and in the low area bunchgrass zones.

The temporal dynamics of the western spruce budworm and mountain pine beetle outbreak show distinct differences between both agents (Fig. 8). For our study area, the mountain pine beetle outbreak began in 2000, peaked in 2007, and decreased afterwards. The current western spruce budworm outbreak also started in 2000 and peaked in 2003. After 2003, infestations by western spruce budworm steadily declined until 2010. Comparing the Landsat based estimates to the temporal profiles of the AOS maps, substantial differences can be observed. The AOS-based area estimates are higher than the Landsat-based estimates, especially for mountain pine beetle. Nevertheless, the temporal patterns of the Landsat based estimates resemble the AOS based trajectories quite well.

5. Discussion

5.1. Mapping mountain pine beetle and western spruce budworm disturbances

5.1.1. Mapping approach

Our results confirm that insect disturbances can be distinguished reliably from undisturbed areas and more intense disturbances such as clear-cut harvest and fire (Goodwin et al., 2008; Kennedy et al., 2012; Meigs et al., 2015), though insect disturbances might be confused with undisturbed areas once disturbance magnitudes are low. This issue was previously reported by other studies (Coops, Wulder, & White, 2006a; Kennedy et al., 2012) and results from the fact that slight disturbances are easily confused with spectral changes caused by residual clouds or phenological differences in the source image stack. Since this confusion results in a higher error of omission for insect disturbances, our resulting insect disturbance map is a more conservative estimation of the total area affected.

We presented evidence that defoliator and bark beetle disturbances can be separated in pure host-stands using spectral and temporal disturbance metrics derived from Landsat time series. However, once mixed stands were considered, there was a high likelihood (44.1%; Table 3) of mountain pine beetle disturbances being falsely attributed.

These errors were predominately located at the border between the Douglas-fir and the lodgepole pine dominated zones, where stands mixed between host- and non-host-trees are common. In those stands, western spruce budworm is the predominant agent of disturbance, but the spectral-temporal signal can be mixed between western spruce budworm and single pines attacked by mountain pine beetle. It is more-over possible that errors in the AOS database are more prevalent in those mixed stands, where different agents are hard to separate visually. Our mixed reference data set might thus include some false labels caused from erroneous attribution the AOS data. Using the VRI information, which is spatially explicit, can help identify stands that are more likely to be classified falsely.

In contrast to the methodological approach suggested by Meigs et al. (2015), which combines LandTrendr with AOS maps using a simple overlay analysis, we used the AOS data to train a model assigning a likelihood of insect agent to each disturbance pixel identified by LandTrendr. Our approach thus allows also attributing agents to insect disturbances outside of AOS polygons. By restricting the training process to those polygons coinciding with host-trees of each insect agent (Franklin et al., 2003), we moreover avoid false attribution by spatially erroneous AOS polygons (i.e. mountain pine beetle AOS polygons in pure Douglas-fir forests; see also Section 5.3).

5.1.2. Spatial and temporal pattern of western spruce budworm and mountain pine beetle disturbances

Our maps show the spatial and temporal patterns of the current outbreaks of mountain pine beetle and western spruce budworm in southern British Columbia, and they spatially expand the maps developed by Meigs et al. (2015) for the USA Pacific Northwest. The spatial patterns of mountain pine beetle and western spruce budworm probability resembled the BEC zones (Fig. 1) and thus the availability of host trees in our study area. Distinct differences in the probability were found for the northern zones (Sub-boreal Pine/Spruce zone) and for the higher elevation zones (Mountain Spruce zone) of the study area, where lodgepole pine is the leading species, and climatic conditions are considered to be less favorable for western spruce budworm. Highest probabilities of western spruce budworm disturbances were found in the lower elevation, hot and dry regions of the Interior Douglas-fir Forest zone, where western spruce budworm is known to be most active (Maclauchlan et al., 2006). In zones mixed between hosts of both insects, however, probabilities of either mountain pine beetle or western spruce budworm were generally lower, indicating that both insects might be present. In those areas, the attribution of one specific agent is thus hampered.

The mountain pine beetle outbreak in our study area started in 2000 and peaked in 2007, whereas the province-wide peak was in

Table 3
Confusion matrix for predicting mountain pine beetle (MPB) and western spruce budworm (WSBW) disturbances in pure and mixed stands.

		Reference				
Map	Agent	WSBW	MPB	Total	User's accuracy [%]	Error of commission [%]
	WSBW	4970	450	5420	91.7	8.3
	MPB	2021	2559	4580	55.9	44.1
	Total	6991	3009			
	Producer's accuracy [%]	71.1	85.0		Overall accuracy [%]	
	Error of omission [%]	28.9	15.0		75.3	

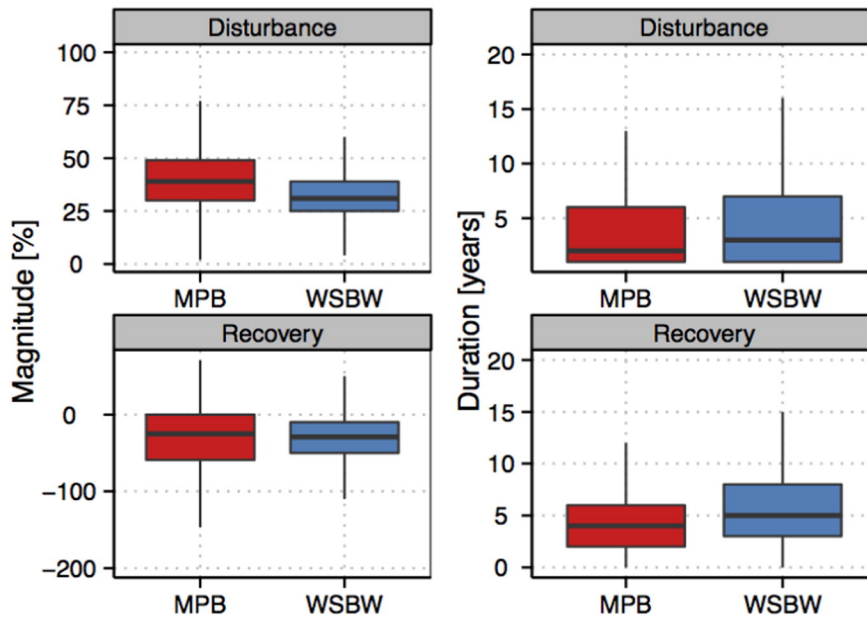


Fig. 5. Boxplots of the disturbance and recovery metrics for the NBR stratified by insect agent. Disturbance and recovery magnitude from NBR are expressed in percent.

2005 (Meddens et al., 2012). Since our study area is located south of the major lodgepole pine areas of British Columbia, the lag to the provincial trends is not unexpected. The western spruce budworm outbreak peaked earlier than mountain pine beetle. There is evidence that drought can influence western spruce beetle population dynamics and trigger outbreaks (Flower, Gavin, Heyerdahl, Parsons, & Cohn, 2014; Hicke et al., 2012), and the drought years 2000–2004 (Schwalm et al., 2012) might be one of the causes for the current outbreak.

Using probability maps instead of discrete class labels allowed for a flexible interpretation of results (Wulder et al., 2006b). Depending on the application, one can choose more conservative or relaxed thresholds, targeting management actions more precisely. Alternatively, it is possible to select the probability threshold based on a selection criteria such as maximized overall accuracy, kappa, or using receiver-operating characteristics (ROC) analysis (Manel, Williams, & Ormerod, 2001).

Even though temporal patterns and trends of mountain pine beetle and western spruce budworm disturbances resembled each other in the Landsat and AOS maps (Fig. 8), we found substantial differences in the actual infestation area estimates (Figs. 7 and 8). Those differences were not unexpected and have been reported previously (e.g., Meigs

et al., 2015), and emerge from the positional issues and the nature of the manual attribution of AOS maps. AOS maps are manually prepared with infestation boundaries often generalized and including areas with non-infested trees or non-vegetated areas. While the Landsat-based estimates might underestimate trace insect disturbances (i.e., single infested trees), the large differences between the Landsat- and AOS based estimates reinforce that area estimates derived from AOS maps must be interpreted with caution (Wulder et al., 2006a).

5.2. Spectral–temporal characteristics of mountain pine beetle and western spruce budworm disturbances

5.2.1. Disturbance magnitude

Spectral change magnitudes were important predictors for distinguishing mountain pine beetle and western spruce budworm disturbances, which is not surprising as it directly relates to the biology and disturbance ecology of the two insects, particularly with respect to disturbance severity and contagiousness. Mountain pine beetle disturbances commonly lead to complete defoliation and mortality within a few years (Wulder et al., 2006a), explaining

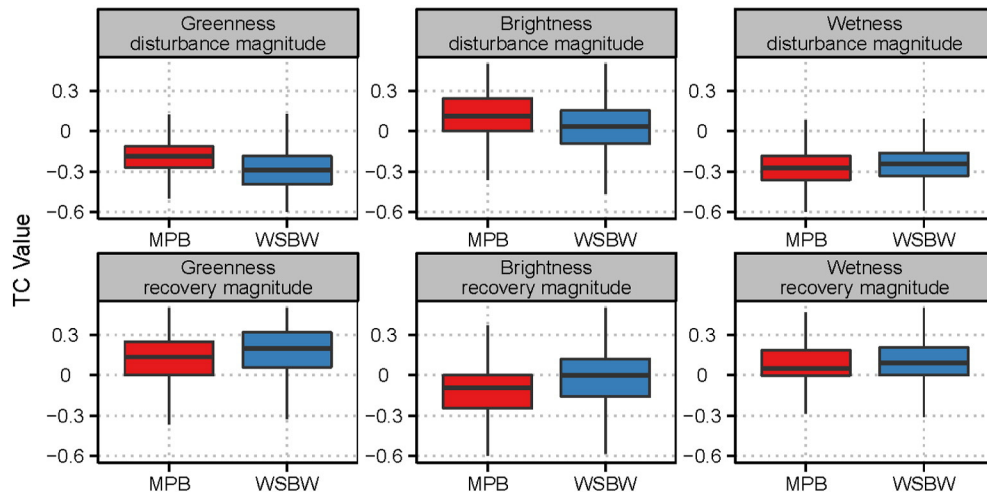


Fig. 6. Boxplots of the disturbance and recovery metrics for the TC components stratified by insect agent. Change magnitudes from TC components are expressed as absolute change in greenness, brightness, and wetness, respectively.

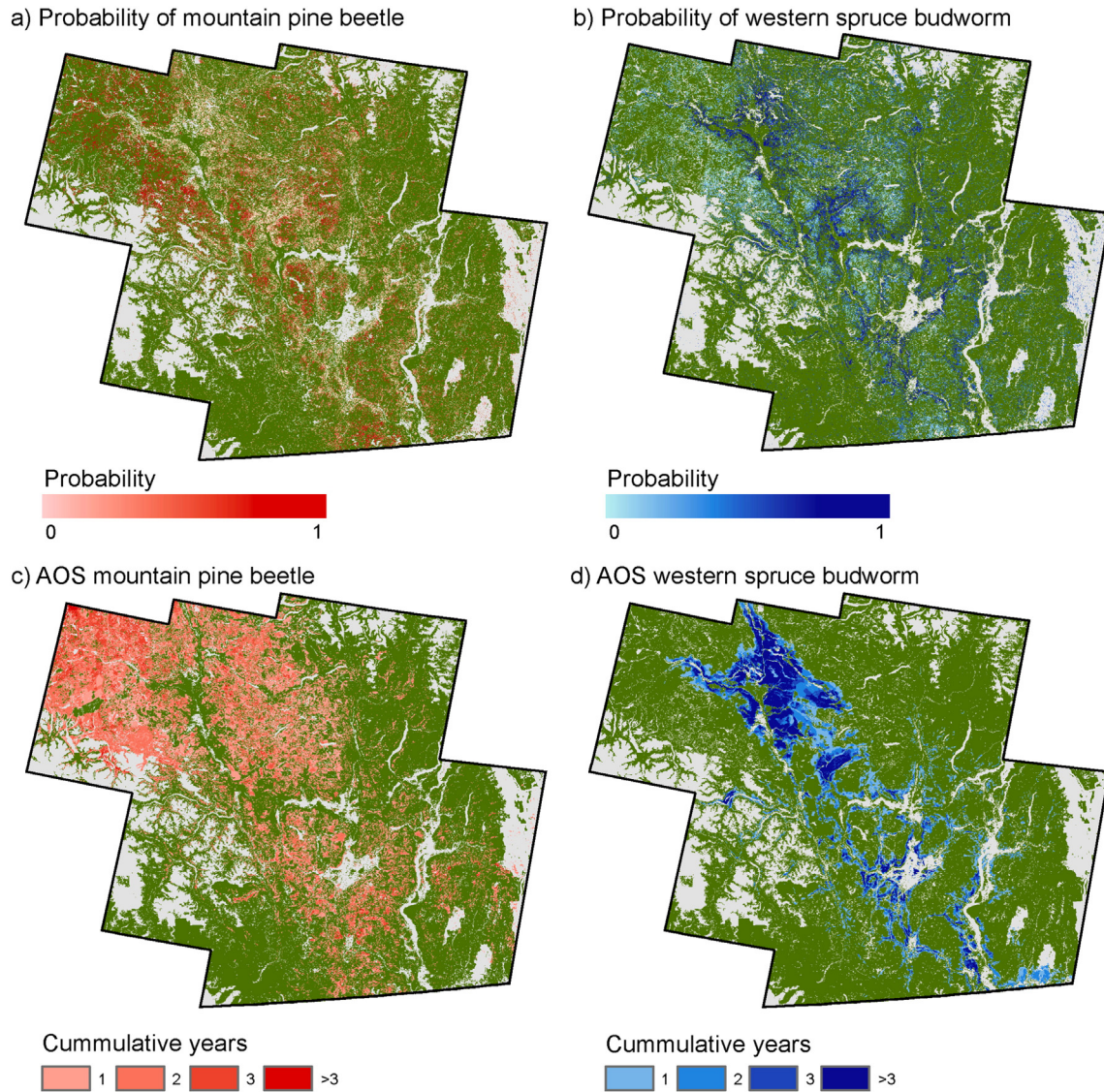


Fig. 7. Mapped probability of (a) mountain pine beetle and (b) western spruce budworm disturbances in comparison to the Aerial Overview Survey (AOS) maps (c and d).

the high spectral change magnitudes associated with mountain pine beetle disturbances. Moreover, mountain pine beetle disturbances commonly occur in aggregated patches (Coops et al., 2010), which facilitates the detection with 30-m Landsat pixels (Meddens, Hicke, Vierling, & Hudak, 2013; Skakun et al., 2003). Infestation patterns by western spruce budworm are often diffuse (Cooke et al., 2007) and result in lower mortality rates, especially if feeding periods are short as in our case (Shepherd, 1994). Nonetheless, trees will show partial symptoms such as chlorosis, deformation, or top-kill (Campbell et al., 2006; Maclauchlan et al., 2006), which also influence the spectral disturbance magnitude. Looking at the VRI database, the rate of dead standing trees (percent of dead trees in relation to dead and alive trees per stand) in Douglas-fir stands affected by western spruce budworm was 15.4% (SD = 4.8%) compared to 44.9% (SD = 28.2%) for lodgepole pine stands affected by mountain pine beetle. Hence, the differences in disturbance magnitude between mountain pine beetle and western spruce budworm disturbances evident in this study can be explained by the different impacts both insects have on tree mortality.

Even though we found expected differences in disturbance magnitude, we also observed an overlap between both insect agents (Fig. 5). Healthy trees present in mixed stands, which dampen the disturbance signal, might cause low disturbance severities for

mountain pine beetle (Skakun et al., 2003). High disturbance severities for western spruce budworm might be the result of western spruce budworm co-occurring with secondary bark beetle (Hummel & Agee, 2003) or drought (Flower et al., 2014). Hence, even though disturbance magnitude was of importance for distinguishing between bark beetle and defoliator disturbances, there is high variability, which complicates the mapping in heterogeneous landscapes where hosts of both insects are present. In our study area, approximately 7% of the lodgepole pine and Douglas-fir stands were comprised a mixture of both host species (i.e., either lodgepole pine or Douglas-fir made up >10% secondary species composition).

The disturbance metrics obtained from the TC components showed a more nuanced picture of the differences between both insect agents than the disturbance metrics obtained from the NBR. The NBR only captured the overall differences in tree mortality, whereas the changes in TC can be attributed to the different impacts both insects have on the tree canopy. The changes in wetness associated with mountain pine beetle can be attributed to the complete defoliation and thus change of the tree canopy caused by mountain pine beetle, which is corroborated by several other studies (Coops, Waring, Wulder, & White, 2009; Franklin et al., 2003; Hais et al., 2009; Skakun et al., 2003; Wulder et al., 2006b). The three times higher changes in brightness for mountain pine beetle disturbances can be attributed to

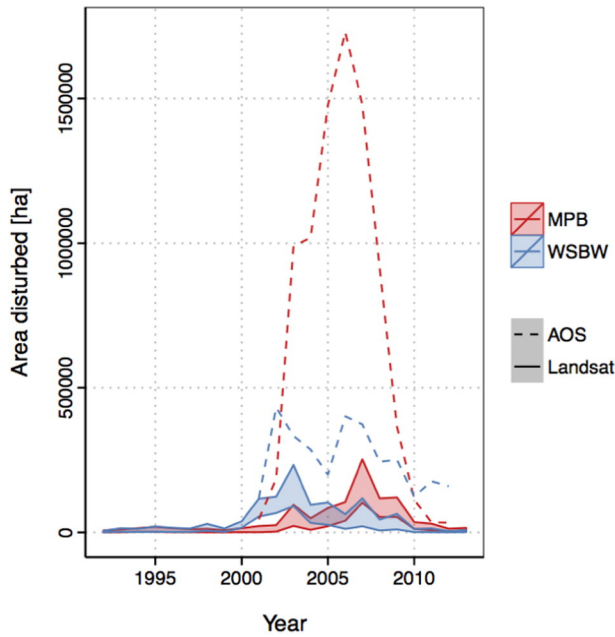


Fig. 8. Temporal dynamics of the western spruce budworm and mountain pine beetle outbreak as estimated from Landsat and the Aerial Overview Survey (AOS) maps. Shown is the area (in hectares) disturbed by one of each insect over time. Landsat estimates are based on different thresholds used for classifying the probability output into presence/absence maps of mountain pine beetle and western spruce budworm. The upper bound represents all stands with a probability greater 0.5 and the lower bound represents all stands with a probability of greater 0.8.

higher bark, branch, and soil reflectance in completely defoliated stands (Hais et al., 2009). As a confounding factor, stands experiencing change at the canopy level can also exhibit stronger understory reflectance (Radeloff et al., 1999). In fact, Hais et al. (2009) found that increasing understory reflectance can increase TC greenness during bark beetle disturbance, which, however, was not the case in our study.

The higher changes in TC greenness associated with western spruce budworm defoliation found in this study might be an indication of the ephemeral changes in foliage, with low impacts on the overall canopy structure of a tree. This result is in agreement with a western spruce budworm outbreak in Oregon (Franklin et al., 1995) and with Gypsy Moth (*Lymantria dispar* Lin.) defoliation in northern Wisconsin (Thayn, 2013). Both studies showed that TC greenness was more important for predicting defoliation than wetness and brightness. A study of the jack pine budworm in Wisconsin (Radeloff et al., 1999) moreover found that changes in green needle fraction, obtained from spectral mixture analysis, had the highest correlation to populations of jack pine budworm.

5.2.2. Disturbance duration

The disturbance duration also showed differences between mountain pine beetle and western spruce budworm, with mountain pine beetle exhibiting mostly short-duration disturbances and western spruce budworm mostly medium- to long-duration disturbances. Mountain pine beetle infestations often follow a three-year scheme (i.e. green-, red-, and gray-attack stage; Goodwin et al., 2008; Wulder et al., 2006a), which is reflected in the high proportion of short-duration disturbances (two years or less) for mountain pine beetle found in this study. For western spruce budworm, the majority of the disturbances were longer than two years, which reflects the common feeding periods of two to five years in our study area (Shepherd, 1994), though we also observed disturbances longer five years. Even though western spruce budworm disturbances tended to be longer than mountain pine beetle disturbances, durations observed in this study were still shorter than durations reported in a study from Oregon

(Meigs et al., 2011). They found more distinct differences in disturbance duration between mountain pine beetle and western spruce budworm and chose a threshold of six years to visually separate both insect agents. For our study, this separation based solely on disturbance duration was not possible, suggesting that a combination of severity and duration metrics achieves best results in separating different insect agents.

5.2.3. Spectral recovery

The spectral recovery signals for western spruce budworm disturbances were generally longer than those for mountain pine beetle infestations. The recovery magnitudes for western spruce budworm disturbances were close the disturbance magnitudes, emphasizing the ephemeral nature of insect defoliation, with often complete regeneration of foliage in the years following the disturbance (Campbell et al., 2006; Cooke et al., 2007). However, understory vegetation also can contribute to the recovery signal by benefiting from the increased light availability in stand experiencing defoliation (Lynch & Moorcroft, 2008). The spectrally faster recovery of lodgepole pine stands may be an indication of such understory tree and shrub vegetation, which capitalizes on increased availability of water, sunlight, and nutrients in mountain pine beetle affected stands. This interpretation is also supported by the rapid changes in brightness following infestation, indicating that soil signals, which are present immediately after infestation, are rapidly covered by understory tree and shrub vegetation.

5.3. Transferability to other regions and uncertainties in the analysis

While this study shows that spectral and temporal patterns of insect disturbances are useful for distinguishing different insect agents, a review of the literature indicates that such patterns can vary by region and outbreak, which means that classification models and logics derived in our study may not be directly transferable to another region. For example, the western spruce budworm outbreak in our study was relatively short and mild, which is typical for this insect (Cooke et al., 2007). However, western spruce budworm impacts can also be more severe if the defoliation lasts over several years or co-occurs with secondary bark beetles. For example, Meigs et al. (2015) found that mountain pine beetle and western spruce budworm generally had equal impacts on tree mortality, which is in contrast to our findings. Differences might result from the relatively light impacts of the current western spruce budworm outbreak compared to past outbreaks in British Columbia (Axelson et al., 2015; Lynch & Moorcroft, 2008) and from differences in regional climate, land use history, and management. For a more severe outbreak, the disturbance magnitudes of mountain pine beetle and western spruce budworm might be less important for distinguishing both insect agents than the disturbance duration (as in Meigs et al. (2011)).

The datasets used in this study have particular strength and weaknesses, introducing uncertainties that need to be considered while transferring methods derived in this study to other regions. First of all, our initial disturbance classification is based on photo-interpretation (i.e. interpretation of Landsat spectral trajectories, image chips, and high-resolution data; Fig. 3), which might be prone to errors. Visually detecting high intensity disturbances such as harvest and fire is relatively easy to achieve, given their significant impact on the Landsat spectral trajectory (Fig. 3). Photo-interpretation has thus been used frequently for labeling reference pixels of such disturbances (Cohen et al., 2010; Kennedy et al., 2012). However, visually detecting transient disturbances, i.e. as caused by light insect disturbances, can be more challenging. We used additional auxiliary data to guide interpretation of insect disturbances, which helped to separate true disturbances from spectral change caused from natural variance in the source stack, i.e. atmospheric noise, residual clouds, phenological differences, or spatial mis-registration.

A second source of uncertainty in the data arises from the AOS maps. Even though the AOS maps are the most comprehensive database on insect disturbances at the landscape level, they are not a precise spatial product. Spatial inaccuracy of the AOS polygons can result from numerous causes, including off-nadir viewing, variations in lighting conditions, and interpreter experience and fatigue, among others (Wulder et al., 2006a). For example, we identified stands where mountain pine beetle was detected even though no host-trees were present according to the VRI database. To account for this potential error in model training, we reduced the selection of training pixels to those pixels where the AOS maps coincided with the respective host tree (Franklin et al., 2003). For validating the model in pure and mixed stands (Table 3), however, we did not apply this filtering step, allowing for a more realistic representation of the landscape (i.e. by including pure and mixed stands). The second validation sample might thus include labeling errors resulting from the AOS dataset. Further research should consider alternative training/validation approaches based on ground-surveys, though for large spatial extents (as in the case of our study), those approaches can be very expensive and time-consuming (Cohen et al., 2010).

6. Conclusion

In this study we characterized bark beetle and defoliator disturbances in southern-interior British Columbia, Canada, using a well-established Landsat-based time series segmentation approach (LandTrendr). From our results, we conclude that Landsat can be utilized to distinguish between bark beetle and defoliation disturbances in our study region, using specific spectral-temporal features. In making the distinction between agents of insect disturbance the magnitude of disturbance was found to be of highest importance. Bark beetle disturbances led primarily to changes in wetness and brightness (i.e., changes in the tree structure such as complete needle loss). Defoliation disturbances were of lower magnitude and linked to changes in greenness (i.e., changes in the trees' foliage). The resulting maps and estimates offer a combined and detailed picture of the mountain pine beetle and western spruce budworm outbreaks in our study region through quantifying both the temporal and spatial dynamics. These otherwise unavailable spatially explicit and quality assured maps can help inform science and management information needs as well as offering new opportunities for addressing increasingly refined forest reporting objectives.

Acknowledgments

Cornelius Senf gratefully acknowledges financial support from the Elsa-Neumann-Stipendium (Elsa Neumann Scholarship) of the Federal State of Berlin. We thank Prof. Robert Kennedy, of Oregon State University, for making LandTrendr freely available (<http://landtrendr.forestry.oregonstate.edu/>). The research presented here contributes to the Global Land Project (<http://www.globallandproject.org>) and the Landsat Science Team (http://landsat.usgs.gov/Landsat_Science_Team_2012-2017.php). Finally, we thank three anonymous reviewers for their very helpful comments.

References

- Alfaro, R. I., Berg, J., & Axelsson, J. (2014). Periodicity of western spruce budworm in southern British Columbia, Canada. *Forest Ecology and Management*, 315, 72–79.
- Alfaro, R. I., Thomson, A. J., & Van Sickle, G. A. (1984). Quantification of Douglas-fir growth losses caused by western spruce budworm defoliation using stem analysis. *Canadian Journal of Forest Research*, 15.
- Alfaro, R. I., Van Sickle, A. J., Thomson, A. J., & Wegwitz, E. (1982). Tree mortality and radial growth losses caused by the western spruce budworm in a Douglas-fir stand in British Columbia. *Canadian Journal of Forest Research*, 12, 780–787.
- Assal, T. J., Sibold, J., & Reich, R. (2014). Modeling a historical mountain pine beetle outbreak using Landsat MSS and multiple lines of evidence. *Remote Sensing of Environment*, 155, 275–288.
- Axelsson, J. N., Smith, D. J., Daniels, L. D., & Alfaro, R. I. (2015). Multicentury reconstruction of western spruce budworm outbreaks in central British Columbia, Canada. *Forest Ecology and Management*, 335, 235–248.
- Breiman, L. (2001). Random forests. *Machine Learning*, 45, 5–32.
- Bright, B. C., Hudak, A. T., Kennedy, R. E., & Meddens, A. J. H. (2014). Landsat time series and Lidar as predictors of live and dead basal area across five bark beetle-affected forests. *IEEE Journal of Selected Topics in Applied Earth Observations and Remote Sensing*, 7, 3440–3452.
- Campbell, R., Smith, D. J., & Arsenault, A. (2006). Multicentury history of western spruce budworm outbreaks in interior Douglas-fir forests near Kamloops, British Columbia. *Canadian Journal of Forest Research*, 36, 1758–1769.
- Cohen, W. B., & Goward, S. N. (2004). Landsat's role in ecological applications of remote sensing. *Bioscience*, 54, 535–545.
- Cohen, W. B., Yang, Z., & Kennedy, R. (2010). Detecting trends in forest disturbance and recovery using yearly Landsat time series: 2. TimeSync – Tools for calibration and validation. *Remote Sensing of Environment*, 114, 2911–2924.
- Cooke, B. J., Nealis, V. G., & Regniere, J. (2007). Insect defoliators as periodic disturbances in northern forest ecosystems. In E. A. Johnson, & K. Miyanishi (Eds.), *Plant disturbance ecology: The process and the response* (pp. 487–525). Burlington, MA: Elsevier.
- Coops, N. C., Gillanders, S. N., Wulder, M. A., Gergel, S. E., Nelson, T., & Goodwin, N. R. (2010). Assessing changes in forest fragmentation following infestation using time series Landsat imagery. *Forest Ecology and Management*, 259, 2355–2365.
- Coops, N. C., Waring, R. H., Wulder, M. A., & White, J. C. (2009). Prediction and assessment of bark beetle-induced mortality of lodgepole pine using estimates of stand vigor derived from remotely sensed data. *Remote Sensing of Environment*, 113, 1058–1066.
- Coops, N. C., Wulder, M. A., & White, J. C. (2006a). Identifying and describing forest disturbance and spatial pattern: Data selection issues and methodological implications. In M. A. Wulder, & S. E. Franklin (Eds.), *Understanding forest disturbance and spatial pattern*. Boca Raton: CRC Press.
- Coops, N. C., Wulder, M. A., & White, J. C. (2006b). Integrating remotely sensed and ancillary data sources to characterize a mountain pine beetle infestation. *Remote Sensing of Environment*, 105, 83–97.
- Core Team, R. (2014). *R: A language and environment for statistical computing*. Vienna, Austria: R Foundation for Statistical Computing.
- Crist, E. P. (1985). A TM tasseled cap equivalent transformation for reflectance factor data. *Remote Sensing of Environment*, 17, 301–306.
- De Beurs, K., & Townsend, P. (2008). Estimating the effect of gypsy moth defoliation using MODIS. *Remote Sensing of Environment*, 112, 3983–3990.
- Flower, A., Gavin, D. G., Heyerdahl, E. K., Parsons, R. A., & Cohn, G. M. (2014). Drought-triggered western spruce budworm outbreaks in the interior Pacific northwest: A multi-century dendrochronological record. *Forest Ecology and Management*, 324, 16–27.
- Franklin, A., Waring, R. H., McCreight, R. W., Cohen, W. B., & Fiorella, M. (1995). Aerial and satellite sensor detection and classification of western spruce budworm defoliation in a subalpine forest. *Canadian Journal of Remote Sensing*, 21, 299–308.
- Franklin, S. E., Fan, H., & Guo, X. (2008). Relationship between Landsat TM and SPOT vegetation indices and cumulative spruce budworm defoliation. *International Journal of Remote Sensing*, 29, 1215–1220.
- Franklin, S. E., Wulder, M. A., Skakun, R. S., & Carroll, A. L. (2003). Mountain pine beetle red-attack forest damage classification using stratified Landsat™ data in British Columbia, Canada. *Photogrammetric Engineering & Remote Sensing*, 69, 283–288.
- Gillanders, S. N., Coops, N. C., Wulder, M. A., Gergel, S. E., & Nelson, T. (2008). Multitemporal remote sensing of landscape dynamics and pattern change: Describing natural and anthropogenic trends. *Progress in Physical Geography*, 32, 503–528.
- Goodwin, N. R., Coops, N. C., Wulder, M. A., Gillanders, S., Schroeder, T. A., & Nelson, T. (2008). Estimation of insect infestation dynamics using a temporal sequence of Landsat data. *Remote Sensing of Environment*, 112, 3680–3689.
- Hais, M., Jonášová, M., Langhammer, J., & Kučera, T. (2009). Comparison of two types of forest disturbance using multitemporal Landsat TM/ETM+ imagery and field vegetation data. *Remote Sensing of Environment*, 113, 835–845.
- Hicke, J. A., Allen, C. D., Desai, A. R., Dietze, M. C., Hall, R. J., Ted Hogg, E. H., ... Vogelmann, J. (2012). Effects of biotic disturbances on forest carbon cycling in the United States and Canada. *Global Change Biology*, 18, 7–34.
- Hope, G. D., Mitchell, W. R., Lloyd, D. A., Erickson, W. R., Harper, W. L., & Wikeen, B. M. (1991). Interior Douglas-fir zone. In D. Meidinger, & J. Pojar (Eds.), *Ecosystems of British Columbia* (pp. 153–166). Victoria, British Columbia, Canada: British Columbia Ministry of Forests.
- Huang, C. Q., Coward, S. N., Masek, J. G., Thomas, N., Zhu, Z. L., & Vogelmann, J. E. (2010). An automated approach for reconstructing recent forest disturbance history using dense Landsat time series stacks. *Remote Sensing of Environment*, 114, 183–198.
- Hummel, S., & Agee, J. K. (2003). Western spruce budworm defoliation effects on forest structure and potential fire behavior. *Northwest Science*, 77, 159–169.
- Kennedy, R., Andréfouet, S., Cohen, W. B., Gómez, C., Griffiths, P., Hais, M., ... Zhu, Z. (2014). Bringing an ecological view of change to Landsat-based remote sensing. *Frontiers in Ecology and the Environment*, 12, 339–346.
- Kennedy, R. E., Yang, Z., & Cohen, W. B. (2010). Detecting trends in forest disturbance and recovery using yearly Landsat time series: 1. LandTrendr – Temporal segmentation algorithms. *Remote Sensing of Environment*, 114, 2897–2910.
- Kennedy, R. E., Yang, Z., Cohen, W. B., Pfaff, E., Braaten, J., & Nelson, P. (2012). Spatial and temporal patterns of forest disturbance and regrowth within the area of the northwest forest plan. *Remote Sensing of Environment*, 122, 117–133.
- Key, C. H., & Benson, N. C. (2006). *Landscape assessment: ground measure of severity, the composite burn index; and remote sensing of severity, the normalized burn ratio. FIREMON: Fire Effects Monitoring and Inventory System*. In *USDA Forest Service General Technical Report RMRS-GTR-164-CD*. Fort Collins: USDA Forest Service Rocky Mountain Research Station.

- Kurz, W. A., Dymond, C. C., Stinson, G., Rampley, G. J., Neilson, E. T., Carroll, A. L., ... Safranyik, L. (2008a). Mountain pine beetle and forest carbon feedback to climate change. *Nature*, 452, 987–990.
- Kurz, W. A., Stinson, G., Rampley, G. J., Dymond, C. C., & Neilson, E. T. (2008b). Risk of natural disturbances makes future contribution of Canada's forests to the global carbon cycle highly uncertain. *Proceedings of the National Academy of Sciences of the United States of America*, 105, 1551–1555.
- Leckie, D. G., & Gillis, M. D. (1995). Forest inventory in Canada with emphasis on map production. *The Forestry Chronicle*, 71, 74–88.
- Liaw, A., & Wiener, M. (2002). Classification and regression by randomForest. *The R Journal*, 2, 18–22.
- Logan, J. A., Régnière, J., & Powell, J. A. (2003). Assessing the impacts of global warming on forest pest dynamics. *Frontiers in Ecology and the Environment*, 1, 130–137.
- Lynch, H. J., & Moorcroft, P. R. (2008). A spatiotemporal Ripley's K-function to analyze interactions between spruce budworm and fire in British Columbia, Canada. *Canadian Journal of Forest Research*, 38, 3112–3119.
- Maclauchlan, L., Brooks, J. E., & Hodge, J. C. (2006). Analysis of historic western spruce budworm defoliation in south central British Columbia. *Forest Ecology and Management*, 226, 351–356.
- Manel, S., Williams, H. C., & Ormerod, S. J. (2001). Evaluating presence–absence models in ecology: The need to account for prevalence. *Journal of Applied Ecology*, 38, 921–931.
- Masek, J. G., Goward, S. N., Kennedy, R. E., Cohen, W. B., Moisen, G. G., Schleeweis, K., & Huang, C. (2013). United States forest disturbance trends observed using Landsat time series. *Ecosystems*, 16, 1087–1104.
- Masek, J. G., Vermote, E. F., Saleous, N. E., Wolfe, R., Hall, F. G., Huemmrich, K. F., ... Teng-Kui, L. (2006). A Landsat surface reflectance dataset for North America, 1990–2000. *Geoscience and Remote Sensing Letters, IEEE*, 3, 68–72.
- Meddens, A. J. H., & Hicke, J. A. (2014). *Spatial and temporal patterns of Landsat-based detection of tree mortality caused by a mountain pine beetle outbreak in Colorado*. USA: Forest Ecology and Management.
- Meddens, A. J. H., Hicke, J. A., & Ferguson, C. A. (2012). Spatiotemporal patterns of observed bark beetle-caused tree mortality in British Columbia and the western United States. *Ecological Applications*, 22, 1876–1891.
- Meddens, A. J. H., Hicke, J. A., Vierling, L. A., & Hudak, A. T. (2013). Evaluating methods to detect bark beetle-caused tree mortality using single-date and multi-date Landsat imagery. *Remote Sensing of Environment*, 132, 49–58.
- Meigs, G. W., Kennedy, R. E., & Cohen, W. B. (2011). A Landsat time series approach to characterize bark beetle and defoliator impacts on tree mortality and surface fuels in conifer forests. *Remote Sensing of Environment*, 115, 3707–3718.
- Meigs, G. W., Kennedy, R. E., Gray, A. N., & Gregory, M. J. (2015). Spatiotemporal dynamics of recent mountain pine beetle and western spruce budworm outbreaks across the Pacific northwest region, USA. *Forest Ecology and Management*, 339, 71–86.
- Nealis, V. (2008). Spruce Budworms, *Choristoneura Lederer* (Lepidoptera: Tortricidae). In J. Capinera (Ed.), *Encyclopedia of Entomology* (pp. 3524–3531). Netherlands: Springer.
- Parker, T. J., Clancy, K. M., & Mathiasen, R. L. (2006). Interactions among fire, insects and pathogens in coniferous forests of the interior western United States and Canada. *Agricultural and Forest Entomology*, 8, 167–189.
- Pflugmacher, D., Cohen, W. B., & Kennedy, R. E. (2012). Using Landsat-derived disturbance history (1972–2010) to predict current forest structure. *Remote Sensing of Environment*, 122, 146–165.
- Pflugmacher, D., Cohen, W. B., Kennedy, R. E., & Yang, Z. (2014). Using Landsat-derived disturbance and recovery history and lidar to map forest biomass dynamics. *Remote Sensing of Environment*, 151, 124–137.
- Pojar, J., Klinka, K., & Meidinger, D. V. (1987). Biogeoclimatic ecosystem classification in British Columbia. *Forest Ecology and Management*, 22, 119–154.
- Radeloff, V. C., Mladenoff, D. J., & Boyce, M. S. (1999). Detecting jack pine budworm defoliation using spectral mixture analysis: Separating effects from determinants. *Remote Sensing of Environment*, 69, 156–169.
- Raffa, K. F., Aukema, B. H., Bentz, B. J., Carroll, A. L., Hicke, J. A., Turner, M. G., & Romme, W. H. (2008). Cross-scale drivers of natural disturbances prone to anthropogenic amplification: The dynamics of bark beetle eruptions. *Bioscience*, 58, 501–517.
- Schoennagel, T., Veblen, T. T., & Romme, W. H. (2004). The interaction of fire, fuels and climate across Rocky Mountain forests. *Bioscience*, 54, 661–676.
- Schwalm, C. R., Williams, C. A., Schaefer, K., Baldocchi, D., Black, T. A., Goldstein, A. H., ... Scott, R. L. (2012). Reduction in carbon uptake during turn of the century drought in western North America. *Nature Geoscience*, 5, 551–556.
- Shepherd, R. F. (1994). Management strategies for forest insect defoliators in British Columbia. *Forest Ecology and Management*, 68, 303–324.
- Skakun, R. S., Wulder, M. A., & Franklin, S. E. (2003). Sensitivity of the thematic mapper enhanced wetness difference index to detect mountain pine beetle red-attack damage. *Remote Sensing of Environment*, 86, 433–443.
- Swetnam, T. W., & Lynch, A. M. (1993). Multicentury, regional-scale patterns of western spruce budworm outbreaks. *Ecological Monographs*, 63, 399–424.
- Thayn, J. B. (2013). Using a remotely sensed optimized disturbance index to detect insect defoliation in the Apostle Islands, Wisconsin, USA. *Remote Sensing of Environment*, 136, 210–217.
- Townsend, P. A., Singh, A., Foster, J. R., Rehberg, N. J., Kingdon, C. C., Eshleman, K. N., & Seagle, S. W. (2012). A general Landsat model to predict canopy defoliation in broadleaf deciduous forests. *Remote Sensing of Environment*, 119, 255–265.
- Vogelmann, J. E., Tolk, B., & Zhu, Z. (2009). Monitoring forest changes in the southwestern United States using multitemporal Landsat data. *Remote Sensing of Environment*, 113, 1739–1748.
- Vogelmann, J. E., Xian, G., Homer, C., & Tolk, B. (2012). Monitoring gradual ecosystem change using Landsat time series analyses: Case studies in selected forest and rangeland ecosystems. *Remote Sensing of Environment*, 122, 92–105.
- Volney, W. J. A., & Fleming, R. A. (2000). Climate change and impacts of boreal forest insects. *Agriculture Ecosystems and Environment*, 82, 283–294.
- Westfall, J., & Ebata, T. (2012). 2012 summary of forest health conditions in British Columbia. In *Pest management report series: Ministry of Forests, Lands and Natural Resource operations*.
- Woods, A. J., Heppner, D., Kope, H. H., Burleigh, J., & Maclauchlan, L. (2010). Forest health and climate change: A British Columbia perspective. *The Forestry Chronicle*, 86, 412–422.
- Wulder, M. A., Dymond, C. C., White, J. C., Leckie, D. G., & Carroll, A. L. (2006a). Surveying mountain pine beetle damage of forests: A review of remote sensing opportunities. *Forest Ecology and Management*, 221, 27–41.
- Wulder, M. A., Masek, J. G., Cohen, W. B., Loveland, T. R., & Woodcock, C. E. (2012). Opening the archive: How free data has enabled the science and monitoring promise of Landsat. *Remote Sensing of Environment*, 122, 2–10.
- Wulder, M. A., White, J. C., Bentz, B., Alvarez, M. F., & Coops, N. C. (2006b). Estimating the probability of mountain pine beetle red-attack damage. *Remote Sensing of Environment*, 101, 150–166.
- Wulder, M. A., White, J. C., Goward, S. N., Masek, J. G., Irons, J. R., Herold, M., ... Woodcock, C. E. (2008). Landsat continuity: Issues and opportunities for land cover monitoring. *Remote Sensing of Environment*, 112, 955–969.
- Wulder, M. A., White, J. C., Grills, D., Nelson, T., Coops, N. C., & Ebata, T. (2009). Aerial overview survey of the mountain pine beetle epidemic in British Columbia: Communication of impacts. *BC Journal of Ecosystems and Management*, 10, 45–58.
- Zhu, Z., & Woodcock, C. E. (2012). Object-based cloud and cloud shadow detection in Landsat imagery. *Remote Sensing of Environment*, 118, 83–94.